J. Chem. Sci. Vol. 127, No. 6, June 2015, pp. 1035–1045.
DOI 10.1007/s12039-015-0861-7

X-H· · · C hydrogen bonds in *n*-alkane-HX (X = F, OH) complexes are stronger than C-H· · · X hydrogen bonds

R PARAJULI[a,*] and E ARUNAN[b]

[a]Department of Physics, Amrit Campus, Tribhuvan University, Kathmandu, Nepal
[b]Department of Inorganic and Physical Chemistry, Indian Institute of Science, Bengaluru 560012, India
e-mail: rparajuli@yahoo.com

MS received 09 October 2014; revised 31 January 2015; accepted 03 February 2015

Abstract. Computational study of X-H· · · C and C-H· · · X hydrogen bonds in *n*-alkane-HX complexes (X=F,OH, alkane=propane, butane, pentane) has been carried out in this work. *Ab initio* and density functional theories were used for this study. For *n*-alkane-H_2O complexes both O· · · H-C and O–H· · · C hydrogen bonded complex have been found, while for *n*-alkane-HF complexes, our attempt to optimize F· · · H-C H-bond was not successful. Like most of the hydrogen bonded systems, strong correlation between binding energy and stretching frequency of H-F and O-H stretching mode was observed. The values of electron density and Laplacian of electron density are within the accepted range for hydrogen bonds. In all these cases, X-H· · · C hydrogen bonds are found to be stronger than C-H· · · X hydrogen bonds.

Keywords. Hydrogen bond; AIM Theory; BSSE correction.

1. Introduction

Methane–water complex has attracted much interest, with a large number of studies focusing on C-H· · · O hydrogen bonding.[1–7] However, microwave spectroscopy has established the structure as having the OH from water pointing towards one of the tetrahedron face of methane.[8] 'Atoms in Molecules' theoretical analysis showed this structure to have O-H· · · C hydrogen bond, and indeed complexes of CH_4 with HF, HCl, HCN and H_2O all have the same interaction.[9] In all these complexes, X-H· · · C hydrogen bonded structure is the global minimum and C-H· · · X hydrogen bonded structure is a local minimum. Unlike the initial days of hydrogen bonding when lone pairs of N, O or F were thought to be the only hydrogen bond acceptors,[10] it has now been recognised that any electron-rich region in a molecule, such as a lone pair, π pair, unpaired electron and sigma electrons, can be hydrogen bond acceptors.[11–14] The recent IUPAC report and recommendation on hydro gen bond have recognised the diverse nature of hydrogen bond donors and acceptors.[13,14]

Unlike methane, hydrogen bonding by higher alkanes has not received much attention. One of the earlier works reported infrared spectroscopic and *ab initio* results but considered only the C-H· · · F-H interaction of CH_4-HF;[15] for the higher alkanes, it did consider the involvement of hydrogen bonding to the C–C single bond.

Akanes, which have been chosen in this work, are simplest organic compounds that contain only two elements, hydrogen and carbon. Each carbon atom forms four bonds and each hydrogen atom forms a single bond to a carbon. The bonding around each carbon atom is tetrahedral, so all bond angles are 109.5°. As a result, the carbon atoms in higher alkanes are arranged in zigzag rather than linear patterns. Alkanes are nonpolar and show relatively low reactivity because their C bonds are stable and cannot be easily broken. Alkanes do not have a lone pair to accept hydrogen bond. But now, any electron-rich region in a molecule can act as a hydrogen bond acceptor. Molecular electrostatic potential is analysed to find the electron-rich region. This approach to identify the sites of electron-rich region was proposed long time ago[16] and has been in use since then.[17–19] A remarkable feature of this technique is that it can be applied for weakly bonded complexes.[20] This approach was subsequently used by Gadre *et al*.[21–24] to elucidate the nature and strength of the bonding involved. Recently, Ragevendra and Arunan have utilized this method to identify regions of high electron density in CH_4[9] and now it is well known that the tetrahedral face of methane has an electron-rich centre and can act as a hydrogen bond accep tor. More recently, the same group with the help of electrostatic potential calculation showed that the opposite face of a tetrahedral group can be made an electron-deficient centre if one of its hydrogen is substituted with some electron-withdrawing group such as F/OH. Discovery of the

*For correspondence

carbon bond is possible even if the molecular electrostatic potential is not analysed. But it can be said definitely that the molecular electrostatic potential surface (MEPS) analysis of CH_3F and CH_3OH was one of the insights for the discovery of carbon bond.[25]

This work aims to explore whether our earlier results on CH_4–HX complexes are extendable to higher alkanes.[9] The proposed O-H$\cdots$C hydrogen bond was observed to lie between a CH_3 group on a silicon surface and adsorbed H_2O molecules.[26] Hammerum *et al.*[27] recently considered alkanes as hydrogen bond acceptors with protonated alcohols/acids as donors.

In this work, hydrogen bonding between neutral HF and H_2O as donors and three alkanes, *n*-propane, *n*-butane and *n*-pentane, are considered. *Ab initio*, densities functional theories, MEPS analysis, atoms in molecules (AIM) theoretical calculation[2,28] are used to investigate these complexes. MEPS analysis is used to identify the sites for hydrogen bond formation and AIM theory is used to characterize the interactions.

2. Computational Methods

The structures of all the molecules and hydrogen-bonded complexes studied in this work were optimized at MP2[30–32] and B3LYP[33–35] levels of theory using 6-311++g** basis set.[36] Meta generalised gradient approximation (meta-GGA) with hybrid meta exchange correlation functionals M05-2X developed by Truhlar's group was also used to optimize these complexes in order to compare MP2 and B3LYP results.[37] Gaussian03 software package was used for all the calculations.[38] The corresponding harmonic frequency calculations were also carried out at the same level to ensure that the complex structures are true minima. The interaction energies were computed by supermolecular approach, and then corrected for the basis set superposition error (BSSE) following the counterpoise procedure proposed by Boys and Bernardi.[39] The AIM calculations were carried out with AIM 2000 package.[40] Gaussian wave functions were used for this. A map of electrostatic potential surface was plotted by using GaussView.[41] Molecular Electrostatic Potential (MESP) of all the acceptors was mapped at 0.001 a.u. electron density isosurface as it encompasses roughly 97% of the molecule's electronic charge.[42] Quantitative analysis of the molecular surfaces of all three alkanes studied here has been carried out using Multiwfn software.[43]

3. Results and Discussion

3.1 *Molecular Electrostatic Potential Surface Analysis of Alkanes*

Figure 1 shows MEPS map of all three alkanes studied in this work. The site of high-electron-density region was known from the map of electrostatic potential surface.

The positions of maximum and minimum values of electrostatic potentials (ESPs) at 0.001 a.u. electron density isosurfaces for all three alkanes are given in Figures 2 and 3.

Tables (S1–S6) given in supporting information show coordinates of nuclear positions and the values of ESP at maximum and minimum positions of all alkanes studied here.

The position of minimum value of ESP has helped to locate the sites of electrophilic attack in this study. From these values of ESP it is found that all carbon atoms can act as hydrogen bond acceptors. To distinguish one carbon atom from another the first carbon atom is designated as *a*, the second *b* and the third *c*.

The calculation of molecular electrostatic potential for alkane was also done by Gadre *et al*. In one of their works, they found the positions of minimum values of ESPs in the middle of the CH_2 group and in the bisector

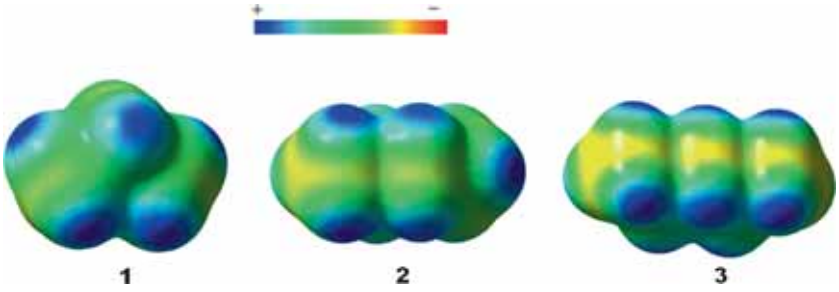

Figure 1. Map of Molecular Electrostatic Potential surface of (1) propane (2), butane (3) and (3) pentane using B3LYP/6-311++G** wave functions. Colour code is: blue, more positive than green, which is more positive than yellow, which is more positive than red. Surfaces were plotted by using GaussView software.

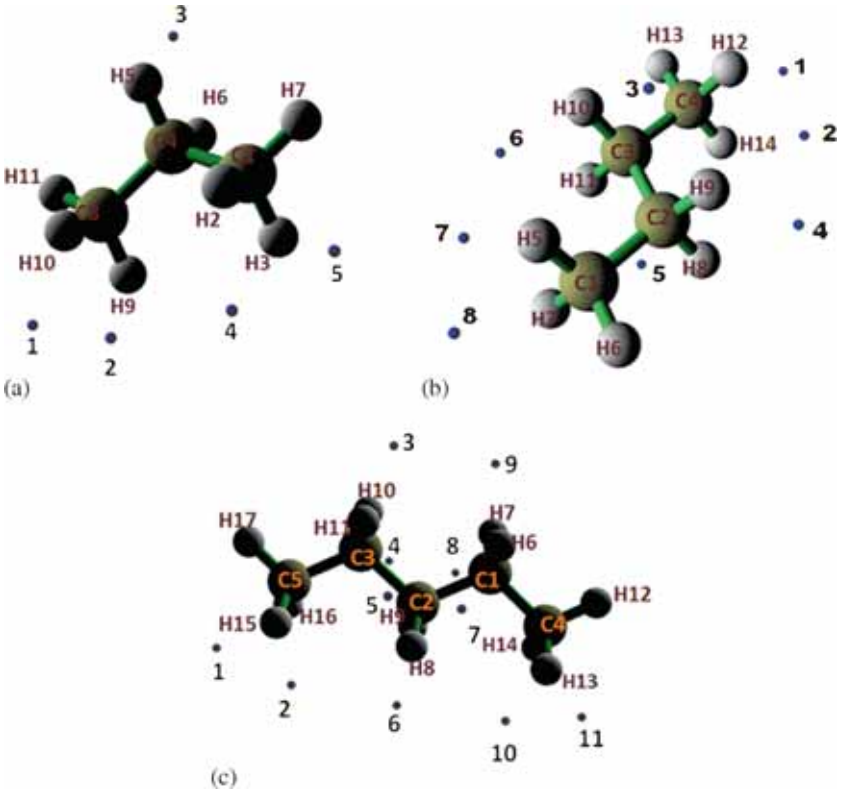

Figure 2. Positions of minimum values of electrostatic potentials (a) propane, (b) butane and (c) pentane optimized at B3LYP/6-311++g**.

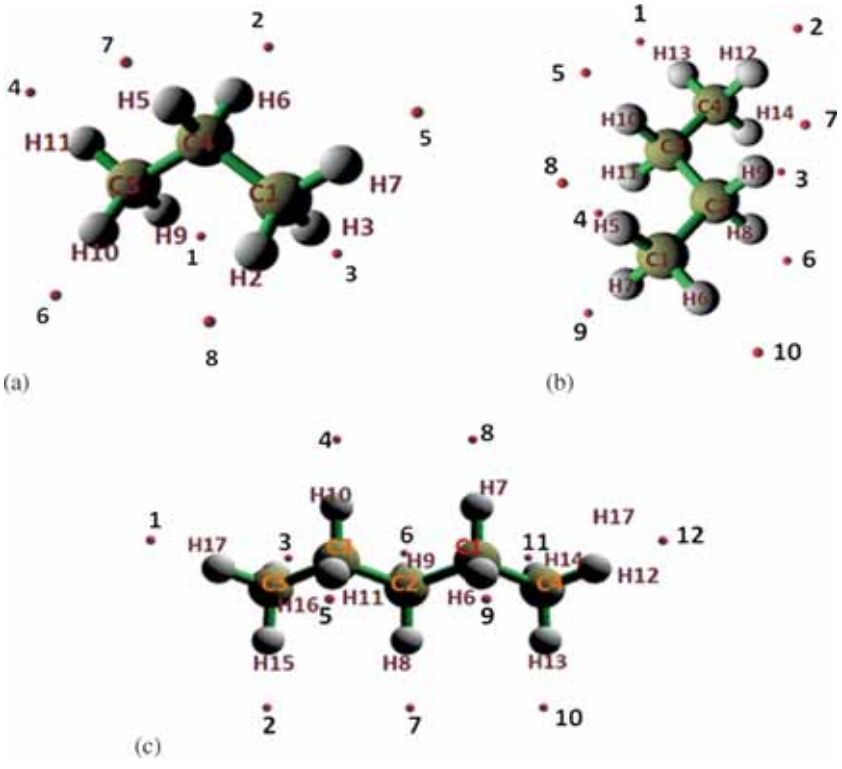

Figure 3. Positions of maximum values of electrostatic potentials: (a) propane, (b) butane and (c) pentane optimized at B3LYP/6-311++g** level.

of the H-C-H angles in the CH_3 terminal group in the case of *n*-butane.[23] We mapped the MEPS and when closely observed the MEPS map, the minimum positions seem to be around the same point as they found. Moreover, figures 4 and 6 clearly indicate that the interaction regions of HF with butane and other alkanes are exactly in the same positions as found by Gadre *et al*.

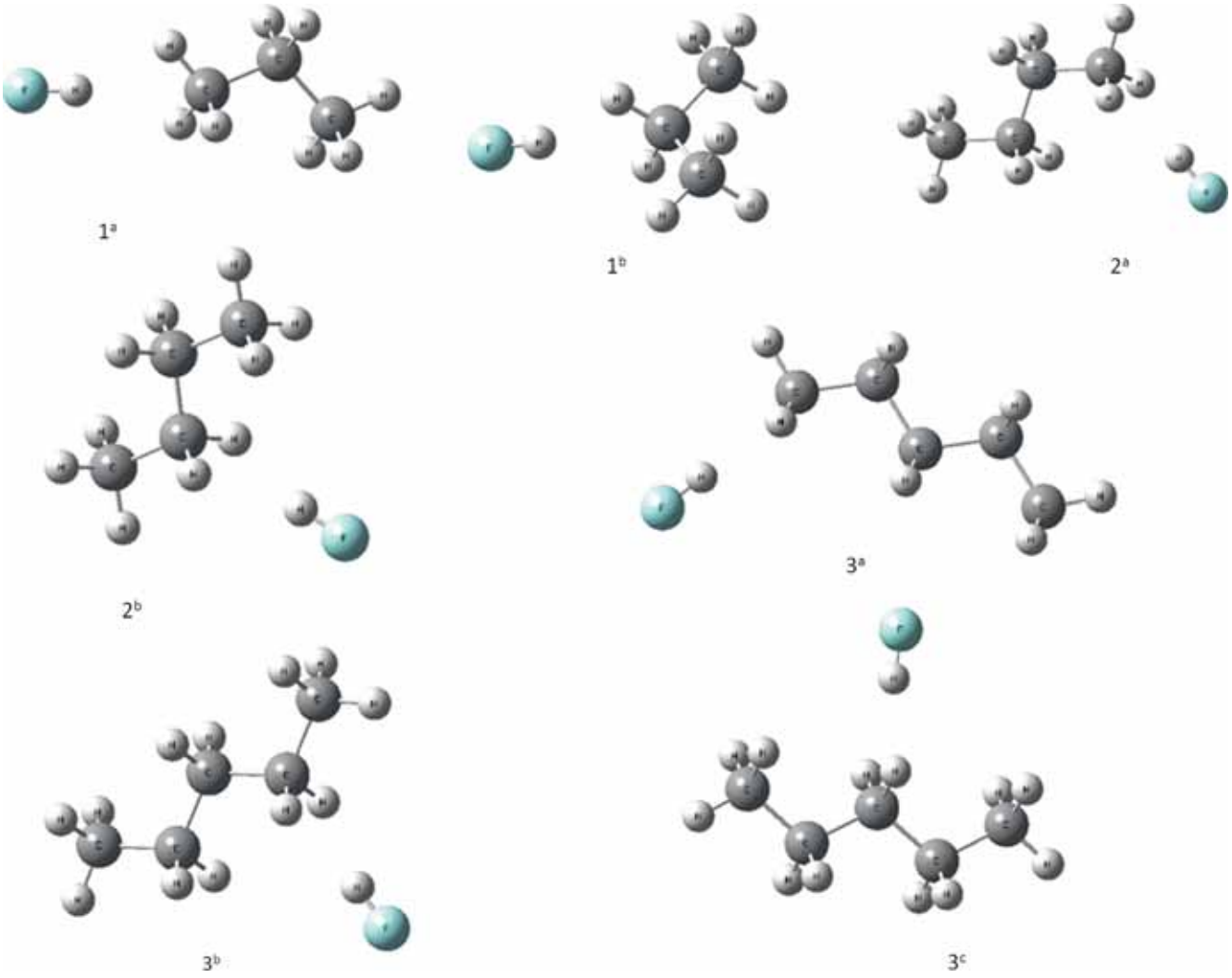

Figure 4. Optimized structure of FH$\cdots$alkane complex. 1 is propane, 2 is butane and 3 is pentane. *a, b* and *c* are three different carbon atoms in B3LYP/6-311++g** level of theory.

Table 1. Optimized H–C bond distances, ∠FHC bond angles, shift in F-H stretching frequency with respect to monomer frequency ($\Delta\upsilon$) in cm^{-1}, change in F-H distance and C-H distance* (Δr) in Å and interaction energy (ΔE) in kJ/mol for F-H $\cdots$ alkane complexes (alkane $\rightarrow$ ^1n-propane, ^2n-butane, ^3n-pentane).

	B3LYP/6-311++G**					MP2/6-311++G**				
	R_{H-C}	∠FHC	Δr	$\Delta\upsilon_{H-F}$	ΔE	R_{H-A}	∠FHC	Δr	$\Delta\upsilon$	ΔE
1[a]	2.4230	177.9	0.0034 0.0027*	−82	−4.5	2.5143	179.7	0.0021 0.0023*	−47	−4.1
1[b]	2.4186	179.2	0.0038 0.0031*	−93	−4.6	2.4637	175.9	0.0024 0.0025*	−58	−4.2
2[a]	2.4386	179.7	0.0037 0.0040*	−86	−4.6	2.5420	174.3	0.0020 0.0025*	−43	−4.3
2[b]	2.4290	178.9	0.0041 0.0035*	−96	−4.9	2.4828	179.6	0.0025 0.0028*	−59	−4.8
3[a#]	2.4122	175.4	0.0035 0.0027*	−82	−4.7	2.4779	175.7	0.0021 0.0021*	−48	−4.2
3[b]	2.4276	176.8	0.0041 0.0032*	−98	−5.0	2.5232	174.6	0.0024 0.0024*	−53	−5.0
3[c]	2.4428	179.4	0.0041 0.0032*	−98	−5.2	2.4688	179.5	0.0029 0.0025*	−67	−5.3

Not fully optimized in MP2 level of theory

3.2 *Geometrical Features, Frequency Shifts, and Interaction for alkane···H-F complexes*

Figure 4 shows the optimized structures of all alkane···H-F complexes and table 1 lists some geometrical parameters. These geometrical parameters include the H–C bond distance, the F–H···C bond angle (∠FHC), the increase in bond length of F–H in the complex compared to the monomer, the vibrational frequency shift in F–H mode following complex formation, and the interaction energy.

The H–C bond distances in all the complexes listed in table 1 were found to be smaller than the sum of the van der Waals radii of the C and H atoms (about 2.9 Å),[10] suggesting the presence of an attractive interaction in these complexes.

In HF–propane complex, this distance is 2.514 Å for the *a* site and it is 2.464 Å for the *b* site at MP2 level of theory, while at B3LYP level it is almost the same (2.423 Å at the *a* site, 2.419 Å at the *b* site). Similar HC distances were observed for HF–butane complexes. In HF–butane, the bond distance for site *a* is 2.439 Å and that for *b*site it is 2.429 Å at B3LYP level of theory. Similar to the HF–propane complex, the bond distances vary at the MP2 level. For *a* sites it is 2.542 Å and for '*b*' sites it is 2.483 Å. However, for the HF–pentane complex this type of trend has not been observed. At B3LYP level of theory, this distance is found to be maximum at site *a* and minimum at site *c*. At MP2 level of theory, maximum value of this distance is at *b* site and minimum value is at *c* site.

One of the geometric criteria of hydrogen bonding is that X-H···A angle must be equal or close to 180°. All the complexes investigated in this work show this directionality. The lowest angle observed for alkane···HF complexes is 174° and the highest is almost 180°.

As expected, the HF bonds are lengthened in all the complexes. The elongation of the HF bond varies from 0.003 to 0.004Å at B3LYP level of theory and 0.002 to 0.003 Å at MP2 level of theory. There is a correlation between these elongations with change in frequency. This elongation is longer than that for hydrogen bonds with sigma acceptor. For hydrogen bonds with sigma acceptor, the elongation on MP2 (full)/6-311++g** level of theory for HF donor is 0.001 Å.[11] However, it is shorter than other types of hydrogen bonds for the same level of theory. For example, with π electron (C_2H_4) acceptor this value is 0.008 Å;[11] with unpaired (CH_3) acceptor it is 0.006 Å,[11] while with lone pairs (H_2O) it is 0.015 Å.[11] Similar elongations have been observed at B3LYP level of theory. The HF bond elongations in site *b* in propane and butane are more than those found at site *a*, and for pentane this is more in site *c*. The above analyses show that the HF bond elongation is completely consistent with the change of the hydrogen bonding distance.

The changes in C–H distances on complex formation are also given in table 1. It seems that mainly two C–H bonds of the CH_3 groups are involved in hydrogen bond formation (figure 4). The C–H distance with one of the C–H bonds of the CH_3 group does not seem to have changed much. For these *n*-alkanes, there are several minima in the ESP and are not situated at the center of the tetrahedron face as found for CH_4 (figure 2).[9] As the minima are closer to two of the CH groups in the terminal CH_3 group we observe elongation of two C–H bonds following H-bond formation and negligible contraction of the third C–H bond. A similar type of elongation of C–H bond was also observed in the work by Olesen *et al*.[17]

Contrary to other geometrical parameters, change in stretching frequency is pronounced and is also correlated with interaction energy and bond elongation. The values reported in table 1 indicate these facts. The shifts in HF frequencies at MP2/6-311++g** level of theory are in the range of 43–67.0 cm^{-1}, which are larger than those of the hydrogen bonds with sigma acceptor. For hydrogen bonds with sigma acceptor (H_2) the shift in HF frequency at MP2(full)/6-311++g** level of theory is 23.9 cm^{-1}.[11] This shift in HF frequencies are found to be lower than that found for other hydrogen bonded systems, for instance, 183 cm^{-111} (230 cm^{-144}) with π electron (C_2H_4) acceptor, 141.6 cm^{-111} (163 cm^{-145}) with unpaired (CH_3) acceptor electron and 346.8 cm^{-111} (364 cm^{-146}) with lone pairs (H_2O) electrons. The values given in the parentheses are experimental values.

The interaction energy is one of the most important measurements for characterizing the intermolecular interaction. The BSSE-corrected interaction energies are presented in table 1. The interaction energies are about 4 kJ/mol at both levels of theory. This value is more than that of sigma (H_2) bonded acceptors and lower than that for hydrogen bonds with other acceptors.[11] We found strong correlation between interaction energy and stretching frequency. This is one of the unique characteristics of a hydrogen bond. It appears that the middle CH_2 group is a better acceptor than the terminal CH_3 group in alkane. Moreover, the approach of hydrogen atom from HF is found to be the position of global minimum structure with the lowest ESP.

The result predicted by B3LYP method is quite similar to that obtained by MP2 method. So, we have carried out calculation using M05-2X functional with 6-311++G** basis set to compare the MP2 and B3LYP results with new DFT functional. Results obtained from this calculation have been summarized in table S7. From this

table, we can conclude that there is no substantially change of ∠FHC bond angles, shift in F-H stretching frequency with respect to monomer frequency, change in F-H distance and C-H distance. However, the difference is more pronounced for H–C bond distance and in the value of interaction energies. When B3LYP results and M05-2X results are compared, the values of interaction energies with M05-2X functional are almost two times more than that obtained by B3LYP. But, there has been in the literature[47] that the level of success of this functional has not been rationalized yet and several important properties are being poorly described.

3.3 *Geometrical Features, Frequency Shifts, and Interaction Energy for Alkane···H2O Complexes with C-H···O and O-H···C Hydrogen Bonds*

Geometrical parameters, that is, hydrogen bond distance, hydrogen bond angle, change in bond length of complex with respect to monomer, change in frequency with respect to monomer and interaction energy for alkane···H-O-H complexes are listed in table 2. These parameters are not as pronounced as in alkane···H-F complexes.

Similar to alkane···H-F (alkane→propane, butane, pentane) complexes, in this study, all three O-H···C complexes were observed. We have observed propane and butane O-H···C complexes in both sites (*a* and *b*), although the structure was not a true minimum at the MP2 level in *b* site in the case of propane. Moreover, we were able to find a true minimum for the pentane···H-O-H complex only at *c* site.

The variation of hydrogen bond distance at B3LYP level of theory is 2.773 Å to 2.859 Å. At MP2 level of theory, the variation is from 2.622 to 2.739. This distance is, of course, less than the sum of van der Waals' radii of carbon and hydrogen atom and the formation of complex is clearly stabilized by O-H···C hydrogen bond. We have obtained very small value of interaction energy (around 1 kJ/mol) in comparison to other hydrogen bonding. However, other parameters like X-H···A angles vary from 163° to173° closer to the linear geometry expected for hydrogen bonds. Although there is very little change of stretching frequency and change in bond length, these parameters are correlated with interaction energy. The red shift in frequency and increase in bond length, however, can justify hydrogen bonding for this system as well.

Changes in C-H distances during complex formation are presented in table 2. In all cases the bond lengthens, and surprisingly there is more increase of C-H distance than O-H distance as in HF···alkane complexes, it seems that mainly two C–H bonds of the CH_3 group are involved for hydrogen bond formation (figure S1). The third C–H bond distance does not change.

H_2O···alkane (C-H···O) interaction was also observed as in methane, although interaction observed in this study were comparatively much weaker than any other hydrogen bonding. Figure 5 shows C-H···O interaction of alkane with water. We present some of the geometrical parameters in the last three rows of table 2. Our results show that the C–H bonds contract slightly, leading to a small blue shift in stretching frequency. As we see in figure 5, it is bifurcated; two H of CH_2 interact with O of H_2O for all alkanes studied here. The interaction energy is quite low as reported in earlier studies (methane with various acceptors),[9] and we also found that alkanes act as very weak donors for hydrogen bonding.

Similar to the alkane···H-F complex, alkane···H-O-H complexes were also optimized at M05-2X/6-311++G** level to compare MP2 and B3LYP results. The relevant values are given in table S8. When these values are compared with MP2 and B3LYP levels, the difference for this complex is found more pronounced than alkane···H-F complex, especially in interaction

Table 2. Optimized H-A bond distances, ∠DHA bond angles, shift in D-H stretching frequency ($\Delta\upsilon$) in cm^{-1}, change in O-H distance and C-H distance* (Δr) in Å and interaction energy (ΔE) in kJ/mol for H-O-H ···alkane complexes (alkane [1]propane [2]butane, [3]pentane). Superscripts with # are alkane ···OH interactions. D is donor atom and A is acceptor atom.

	B3LYP/6-311++G**					MP2/6-311++G**				
	R_{H-A}	∠DHA	Δr	$\Delta\upsilon$	ΔE	R_{H-A}	∠DHA	Δr	$\Delta\upsilon$	ΔE
1[a]	2.7975	162.5	0.0007 0.0020*	−3	−1.2	2.6867	175.5	0.0007 0.0021*	−4	−2.4
1[b]	2.7916[$]	172.1	0.0009 0.0015*	−7	−1.1	2.7168	171.925	0.0008 0.0016	−6	−2.2
2[a]	2.7728	163.6	0.0008 0.0020*	−4	−1.3	2.6216	168.5	0.0008 0.0010*	−5	−2.5
2[b]	2.8592	173.1	0.0009 0.0013*	−6	−1.2	2.7386	172.3	0.0009 0.0012*	−6	−3.1
3[c]	2.8484	176.2	0.0009 0.0025*	−6	−1.3	2.7070	170.5	0.0011 0.0010*	−9	−3.4
1b[#]	2.7512	150.5	−0.0011	2	−0.7					
2[b#]	2.7616	152.3	−0.0012	4	−0.6					
3[b#]	2.7664	152.2	−0.0015	3	−0.5					

$ Not fully optimized at MP2 level of theory

energy and change in stretching frequency of complex with respect to monomer frequency. In the C···O-H alkane complex at MP2 and B3LYP levels, increase in bond length with red shift in frequency was observed. But at M05-2X level for the same complex, increase in bond length with blue shift in frequency was found.

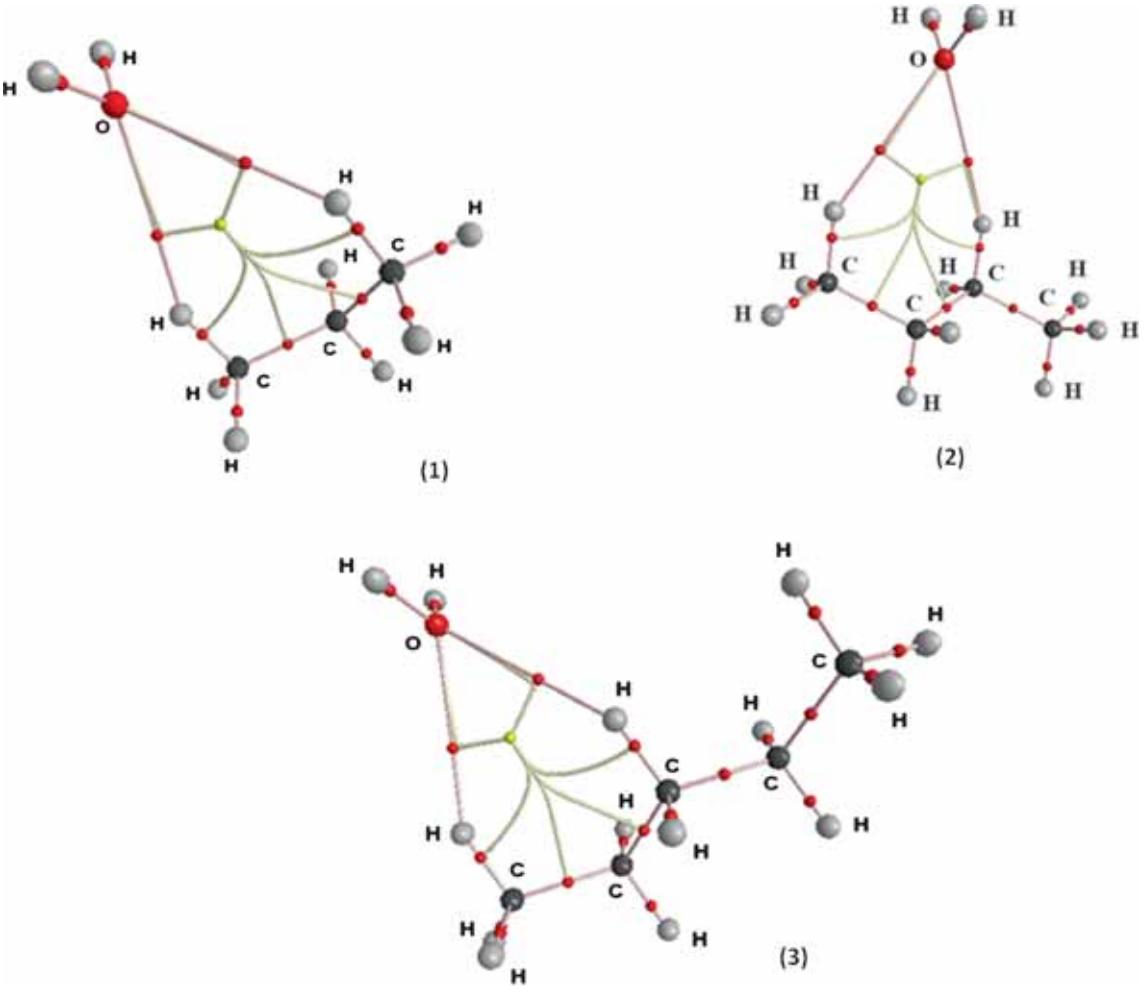

Figure 5. Molecular graph of H_2O–alkane complex for C-H···O interaction at B3LYP/6-311++g** level (1) propane, (2) butane and (3) pentane.

Table 3. Change in Gibbs free energy ΔG during complex formation of X-H···C and C-H···X (X=F, OH) complexes at 298.15 K and 1 atm pressure and 0.001 K and 1 atm pressure* calculated on the basis of harmonic vibrational frequency calculation with basis set 6-311++g**.

		ΔG in kcal/mol					ΔG in kcal/mol		
		B3LYP		MP2			B3LYP		MP2
Complex	Site	298.15$^{\$}$	0.001$^{\$}$	298.15$^{\$}$	Complex	site	298.15$^{\$}$	0.001$^{\$}$	298.15$^{\$}$
$C_3H_8\cdots HF$	a	4.83	−0.40	4.76	$C_3H_8\cdots HOH$	a	3.90	−0.08	3.19
	b	4.57	−0.47	3.51		b	3.97	−0.17	5.35
						C-H···O	4.23	−0.03	2.90
$C_4H_{10}\cdots HF$	a	5.44	−0.47	5.02	$C_4H_{10}\cdots HOH$	a	4.24	−0.03	3.37
	b	5.62	−0.54	4.95		b	4.34	0.04	4.41
						C-H···O	5.12	−0.06	4.08
$C_5H_{12}\cdots HF$	a	5.46		6.52	$C_5H_{12}\cdots HOH$	c	3.81	0.15	4.45
	b	5.34		4.90		C-H···O	4.73	−0.01	3.11
	c	5.49		4.68					

$ represents temperature in Kelvin.

Table 4. Electron density (ρ), the Laplacian (L→-1/4$\nabla^2\rho$) values at the HBCP in atomic units (a.u.), penetration parameter of acceptor and hydrogen (Δr_A, Δr_H) in Å for F-H · · · alkane complexes.

Complex		B3LYP/6-311++G**				MP2/6-311++G**			
		ρ	L	Δr_A	Δr_H	ρ	L	Δr_A	Δr_H
1	A	0.0106	−0.0010	0.610	0.311	0.0086	−0.0085	0.551	0.273
	B	0.0115	−0.0106	0.482	0.322	0.0010	−0.0099	0.451	0.298
2	A	0.0108	−0.0099	0.569	0.312	0.0083	−0.0075	0.459	0.251
	B	0.0113	−0.0104	0.472	0.319	0.0097	−0.0094	0.434	0.292
3	A	0.0106	−0.0100	0.615	0.311	0.0091	−0.0086	0.578	0.279
	B	0.0113	−0.0104	0.478	0.320	0.0089	−0.0081	0.425	0.269
	C	0.0120	−0.0101	0.476	0.315	0.0104	−0.0095	0.463	0.300

(1)FH—C_3H_8, (2)FH—C_4H_{10} (3)FH—C_5H_{12}

Table 5. Electron densities and the Laplacian (L→-1/4$\nabla^2\rho$) values at the HBCP for water· · · alkane complexes in atomic units.

Complex		B3LYP/6-311++G**				MP2/6-311++G**			
		ρ	L	Δr_A	Δr_H	ρ	L	Δr_A	Δr_H
1	A	0.00483	−0.00410	0.466	0.852	0.00603	−0.00545	0.292	0.905
	b[$]	0.00584	−0.00485	0.519	0.911	0.00679	−0.00598	0.332	0.931
2	A	0.00531	−0.00432	0.449	0.859	0.00616	−0.00577	0.483	0.915
	B	0.00496	−0.00409	0.267	0.876	0.00624	−0.00548	0.219	0.649
3	C	0.00531	−0.00432	0.287	0.884	0.00686	−0.00599	0.350	0.929
1#		0.00544	−0.00423	0.221	0.526				
2#		0.00540	−0.00418	0.216	0.440				
3#		0.00530	−0.00411	0.210	0.314				

$ Not fully optimized in MP2 level of theory

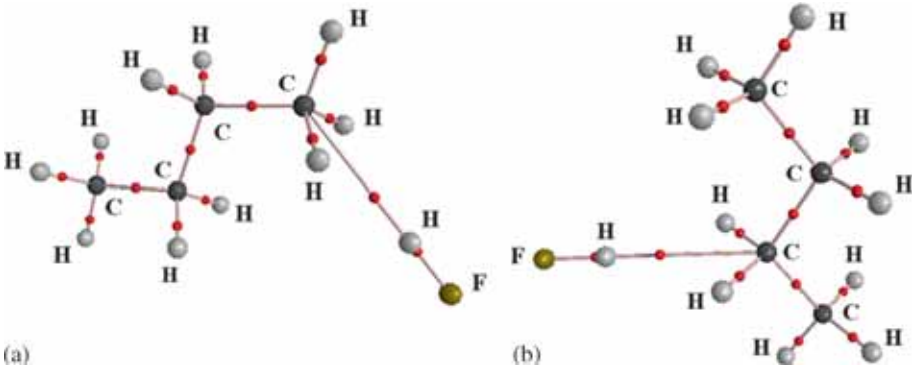

Figure 6. Molecular graph of FH—butane complex at B3LYP/6-311++g** level for (a) first carbon atom and; (b) second carbon atom.

3.4 *Gibbs Free Energy*

To check the stability of this complex we calculated the change in Gibbs free energy (ΔG). This calculation was done on the basis of the harmonic vibration frequency calculations.[48] ΔG was calculated at temperature 298.15 K and 0.001 K by fixing the pressure at 1 atm. As the computational cost in frequency calculations is very high especially in MP2 level of theory, we performed this calculation only at B3LYP level of theory for 0.0001 K temperature. These complexes chosen for this study are weak. So, as expected, these complexes are unstable at 298.15 K temperature and 1 atmospheric pressure from a thermochemical point of view. Table 3 justifies this. However, it can be seen from the same table that at 0.001 K all alkane· · · HF complexes are stabilized. But, in case of alkane· · · H-O-H complex, only butane· · · H-O-H complex (C· · · H-O) at b site and pentane· · · H-O-H complex (C· · ·H-O) at c site are stable from a thermochemical point of view at the same temperature.

3.5 *AIM Theoretical Analysis*

The quantum theory of atoms in molecules (AIM) is widely used for understanding inter- and intra-molecular interactions.[28] The presence and characteristics (electron densities and Laplacian) of a hydrogen bond critical point (HBCP) has been quite useful in characterizing a hydrogen bond.[29] Hence, the properties at the HBCPs have been analyzed in terms of the electron density (ρ) and its Laplacian ($\nabla^2\rho$) for the complexes studied here. The results are compiled in tables 4 and 5.

Figures 6 and 7 show the optimized structures and electron density critical points for butane$\cdots$HF complex and butane$\cdots$water complex. The values of the electron densities lie in the range of 0.01063 to 0.01200 a.u. for alkane$\cdots$HF complexes at B3LYP level of theory, and at MP2 level of theory this range is from 0.00864 to 0.01045 a.u.

The electron density at the HBCPs has a strong correlation with binding energy.[49] Based on this correlation the middle carbon atoms form stronger hydrogen bonds than the corner atoms. This observation is consistent with MESP values as well. Tables 4 and 5 show that this is valid for all the three systems studied. The last three rows of table 5 give the data for the value of electron density and Laplacian of electron density when C–H acts as a hydrogen bond donor. These values are within the commonly accepted values for hydrogen bonds, thus showing the typical closed-shell interactions in these complexes. According to Koch and Popelier,[29] mutual penetration of H and acceptor atoms is a necessary and sufficient condition. These parameters (Δr_A and Δr_H) are also listed in table 4, namely, the difference between non-bonded and bonded radii of the acceptor and hydrogen atoms, measuring the extent of penetration of electron cloud. The bonded radius is the distance from the bonded atom to the bond critical point along the bond path. The non-bonded radius is calculated as the distance from the atom to the point at which the electron density becomes 0.001 a.u. along the bond path in the isolated molecule. The bonded radii and the non-bonded radii are listed in the supporting material. The other parameters given by Koch and Popelier, such as change in atomic volume, ΔV; change in total atomic energy, ΔE; and change in atomic first moments, ΔM, all for the H-bonded hydrogen atom all satisfy the criteria for these interactions to be classified as hydrogen bonds (See Supplementary Information). However, the change in atomic population, ΔN, shows an exception like in an earlier report on $H_4C\cdots HX$ complex.[9]

As mentioned already, AIM analyses have also been applied to the study of H-O-H$\cdots$alkane complexes.

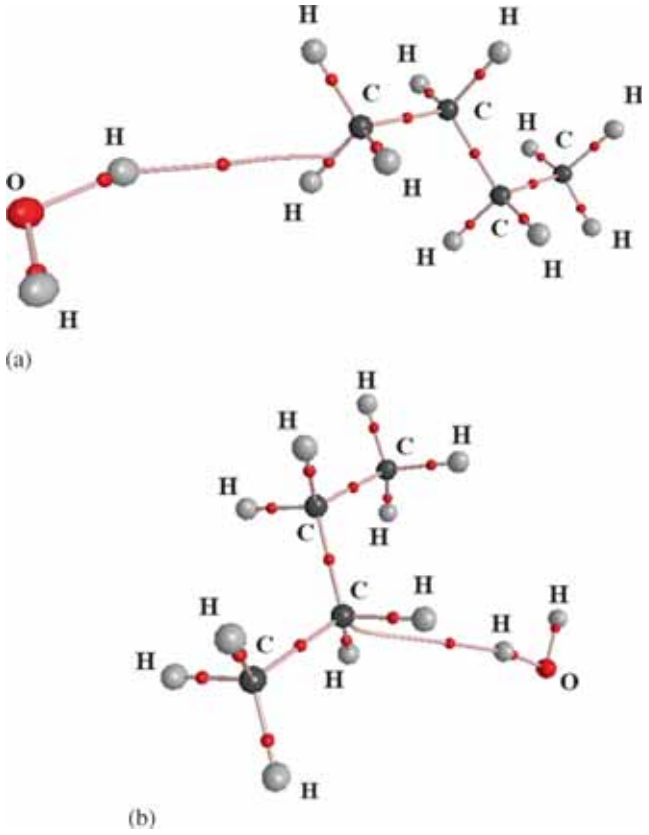

Figure 7. Molecular graph of Water $\cdots$butane complex B3LYP level of theory for (a) first carbon atom and; (b) second carbon atom.

According to Koch and Popelier,[29] among the eight criteria for the assessment of the existence of a hydrogen bond, the most important one is the existence of an HBCP. The existence of HBCP is clearly seen in figure 7. Table 4 shows that the values of the electron density and its Laplacian fall within the proposed range for the hydrogen bond (0.002–0.035 a.u. for the electron density and 0.024–0.139 a.u. for the Laplacian) and the value of electron density in all cases is near to 0.005 a.u. and the value of Laplacian is nearly 0.024. Mutual penetration of H and acceptor atoms for $H_2O\cdots$alkane complex has also been calculated as listed in table 5.

4. Conclusion

Alkane as hydrogen bond acceptor has been characterised using MEPS, *ab initio* (MP2/6-311++G(d,p)), DFT (B3LYP/6-311++G(d,P) and MO5-2X/6-311++G(d,P)) and AIM theoretical calculations. Accompanied with the elongation of HF bond and OH bonds, the complex exhibits a red shift of the HF and OH stretching frequencies. There is change in C–H

bond length as well. The binding energies of the complex range from 1 to 9 kJ/mol. It appears that mainly two C–H bonds participate for hydrogen bonding in CH_3 group. AIM theory also supports this type of interaction. Our attempts to optimize the geometry for alkane$\cdots$H-F complexes in which the alkane is the hydrogen bond donor was not successful. However, for a $H_2O\cdots$alkane complex, very weak interaction has been found when H of alkane (O$\cdots$H-C) is hydrogen bond donor. From this study we can say that X-H$\cdots$C hydrogen bonds in *n*-alkane-HX (X = F, OH) complexes are stronger than C-H$\cdots$X hydrogen bonds.

Supplementary Information

Supplementary information is available at www.ias.ac.in/chemsci. In table S1, coordinate of propane optimized at B3LYP/6-311++g** is given. Positions of maximum and minimum values of ESPs and the values of ESPs are given in S2. The corresponding values for butane and pentane are given in tables S3, S4, S5 and S6, respectively. Some relevant parameters optimized with M05-2X/6-311++G** level of theory of the complex are presented in tables S7 and S8. Penetration parameters, bonding radius of acceptor, non-bonding radius of hydrogen atom, bonding radius of hydrogen atom are given in table S9. Changes in atomic volumes, populations, and energies are given in tables S10, S11 and S12, respectively. In table S13, changes in atomic first moments of the "H" of F-H$\cdots$alkane complexes are given. The optimized structure of Water$\cdots$alkane complex at B3LYP/6-311++g** level of theory is given in figure S1.

Acknowledgements

RP thanks Academy of Science for Developing World for TWAS-UNESCO Associateship, Prof. Rangarajan, the then Chairman, International Relation Cell, Indian Institute of Science and all the lab-members of Prof. Arunan's laboratory. We thank the Supercomputer Education Research Centre at the Indian Institute of Science for computational facilities. RP would like to acknowledge Prof E Krishnakumar and Tata Institute of Fundamental Research (TIFR), Mumbai, India, for the visiting scientist position in January 2013 and January 2015 where the final form of this manuscript was prepared and revised. RP also acknowledges Centre for Science and Technology of the Non-Aligned and Other Developing Countries (NAM S&T Centre), New Delhi, for providing travel grants to visit TIFR in January 2015 and Dr. Leela Pradhan Joshi, Department of Physics, Amrit Campus, Tribhuvan University.

References

1. Szczęśniak M M, Chałasiński G, Cybulski S M and Cieplak P 1993 *J. Chem. Phys.* **98** 3078
2. Novoa J J and Tarron B 1991 *J. Chem. Phys.* **95** 5179
3. Rovira C and Novoa J J 1997 *Chem. Phys. Lett.* **279** 140
4. Kozmutza C, Varga I and Udvardi L 2003 *Theochem* **666–667** 95
5. Hartman M, Wetmore S D and Radom L 2001 *J. Phys. Chem. A* **105** 4470
6. Novoa J J, Planas M and Carme Rovira M 1996 *Chem. Phys. Lett.* **251** 33
7. Ojo O A and Szalewicz K 2005 *J. Chem. Phys.* **123** 134311
8. Suenram R D, Fraser G T, Lovas F J and Kawashima Y J 1994 *Chem. Phys.* **101** 7230
9. Raghavendra B and Arunan E 2008 *Chem. Phys. Lett.* **467** 37
10. Pauling L 1960 In *The Nature of the Chemical Bond and the Structure of Molecules and Crystals, An Introduction to Modern Structural Chemistry* (NY: Cornell University Press Ithaca) p. 478
11. Raghavendra B and Arunan E 2007 *J. Phys. Chem. A* **111** 9699
12. Hammerum S 2009 *J. Am. Chem. Soc.* **131** 8627
13. Arunan E, Desiraju G R, Klein R A, Sadlej J, Scheiner S, Alkorta I, Clary D C, Crabtree R H, Dannenberg J J, Hobza P, Kjaergaard H G, Legon A C, Mennucci B and Nesbitt D J 2011 *Pure Appl. Chem.* **83** 1619
14. Arunan E, Desiraju G R, Klein R A, Sadlej J, Scheiner S, Alkorta I, Clary D C, Crabtree R H, Dannenberg J J, Hobza P, Kjaergaard H G, Legon A C, Mennucci B and Nesbitt D J 2011 *Pure Appl. Chem.* **83** 1637
15. Davis S R and Andrews L 1987 *J. Am. Chem. Soc.* **109** 4768
16. Bonaccorsi R, Scrocco E and Tomasi J 1970 *J. Chem. Phys.* **52** 5270
17. Politzer P 1981 In *Chemical Applications of Atomic and Molecular Electrostatic Potential* D G Truhlar (ed.) (New York: Plenum), pp. 1–6
18. Gadre S R and Shirsat R N 2000 In *Electrostatics of Atoms and Molecules* (Hyderabad: Universities Press (India) Ltd.) p. 63
19. Politzer P, Murray J S and Clark T 2010 *Phys. Chem. Chem. Phys.* **12** 7748
20. Gadre S R and Bhadane P K 1997 *J. Chem. Phys.* **107** 5625
21. Gadre S R and Pathak R K 1990 *Proc. Indian Acad. Sci. (J. Chem. Sci.)* **102** 189
22. Chandra A K, Pal S, Limaye A C and Gadre S R 1995 *Chem. Phys. Lett.* **247** 95
23. Gadre S R and Pingale S S 1998 *J. Am. Chem. Soc.* **120** 7056
24. Gadre S R and Bhadane P K 1998 *Theor. Chem. Acc.* **100** 300
25. Mani D and Arunan E 2013 *Phys. Chem. Chem. Phys.* **15** 14377
26. Ambrosetti A, Costanzo F and Silvestrelli P L 2011 *J. Phys. Chem. C* **115** 12121
27. Olesen S G and Hammerum S 2009 *J. Phys. Chem. A* **113** 7940

28. Bader R F W 1990 In *Atoms in Molecules: A Quantum Theory* (Oxford: Clarendon Press)
29. Koch U and Popelier P L A 1995 *J. Phys. Chem.* **99** 9747
30. Chr Møller and Plesset M S 1934 *Phys. Rev.* **46** 618
31. Pople J A, Raghavachari K, Schlegel H B and Binkley J S 1979 *Int. J. Quantum Chem., Quant. Chem. Symp.* **S13** 225
32. Head-Gordon M, Pople J A and Frisch M J 1988 *Chem. Phys. Lett.* **153** 503
33. Becke A D 1993 *J. Chem. Phys.* **98** 5648
34. Lee C, Yang W and Parr R 1988 *Phys. Rev. B* **37** 785
35. Stephens P J, Devlin F J, Chabalowski C F and Frisch M J 1994 *J. Phys. Chem.* **98** 11623
36. Frisch M J, Pople J A and Stephen Binkley J 1984 *J. Chem. Phys.* **80** 3265
37. Zhao Y, Schultz N E and Truhlar D G 2006 *J. Chem. Theory Comput.* **2** 364
38. Frisch M J, Trucks G W, Schlegel H B, Scuseria G E, Robb M A, Cheeseman J R, Montgomery J A Jr, Vreven T, Kudin K N, Burant J C, Millam J M, Iyengar S S, Tomasi J, Barone V, Mennucci B, Cossi M, Scalmani G, Rega N, Petersson G A, Nakatsuji H, Hada M, Ehara K, Toyota K, Fukuda R, Hasegawa J, Ishida M, Nakajima T, Honda Y, Kitao O, Nakai H, Klene M, Li X, Knox J E, Hratchian H P, Cross J B, Adamo C, Jaramillo J, Gomperts R, Stratmann R E, Yazyev O, Austin A J, Cammi R, Pomelli C, Ochterski J W, Ayala P Y, Morokuma K, Voth G A, Salvador P, Dannenberg J J, Zakrzewski V G, Dapprich S, Daniels A D, Strain M C, Farkas O, Malick D K, Rabuck A D, Raghavachari K, Foresman J B, Ortiz J V, Cui Q, Baboul A G, Clifford S, Cioslowski J, Stefanov B B, Liu G, Liashenko A, Piskorz P, Komaromi I, Martin R L, Fox D J, Keith T, Al-Laham M A, Peng C Y, Nanayakkara A, Challacombe M, Gill P M W, Johnson B, Chen W, Wong M W, Gonzalez C and Pople J A, *Gaussian 03, revision E.01, Gaussian, Inc*, Wallingford, CT (2004)
39. Boys S B and Bernardi F 1970 *Mol. Phys.* **19** 553
40. Biegler-Konig F, Schonbohm J, Derdau R, Bayles D and Bader R F W, *AIM 2000, version 1*, Büro für Innovative Software, Bielefeld, Germany (2000)
41. Dennington R, Keith T and Millam J, *GaussView, Version 5*, Semichem Inc., Shawnee Mission KS (2009)
42. Bader R F W, Carroll M T, Cheeseman J R and Chang C 1987 *J. Am. Chem. Soc.* **109** 7968
43. Lu T and Chen F 2012 *J. Comput. Chem.* **33** 580
44. Huang Z Z and Miller R E 1988 *J. Phys. Chem.* **92** 46
45. Merrit J M, Rudic S and Miller R E 2006 *J. Chem. Phys.* **124** 084301
46. Bulychev V P, Gromova E I and Tokhadge K G 2004 *Opt. Spectrosc.* **96** 774
47. Sousa S F, Fernandes P A and Ramos M J 2007 *J. Phys. Chem. A* **111** 10439
48. http://www.gaussian.com/g_whitepap/thermo.htm
49. Shahi A and Arunan E 2014 *Phys. Chem. Chem. Phys.* **16** 22935